POLYMER ASSISTED COMBUSTION SYNTHESIS OF La-DOPED ZnO NANOPARTICLES - STRUCTURAL, THERMAL, OPTICAL, MORPHOLOGICAL STUDIES

V. S. SAI KUMAR[a], K. V. RAO[b*]
[a]*Department of Physics,.Guru Nanak Institute of Technology, Ibrahimpatnam, 501510, Telangana, India.*
[b]*Centre for Nano Science and Technology, Institute of Science and Technology, Jawaharlal Nehru Technological University Hyderabad, Hyderabad 500085, Telangana, India.*

In this work, La-doped Zinc oxide ($La_xZn_{1-x}O$, *x= 0.0, 0.02, 0.04, 0.06, 0.08 and 0.1*) nanoparticles were successfully prepared by polymer assisted combustion synthesis from the precursor materials like lanthanum nitrate, zinc nitrate, glycine and polyvinyl alcohol in aqueous solutions. La-doped ZnO nanoparticles obtained were further calcined at 400^0C. The effects of adding lanthanum dopant to the ZnO nanoparticles with variations in their properties were studied by X-Ray Diffraction (XRD), Thermo gravimetric/Differential Thermal Analyzer (TG-DTA),UV–vis spectrophotometer, Scanning electron microscope (SEM) and Transmission electron microscope (TEM). The XRD results indicated that the synthesized La-doped ZnO nanoparticles had the pure wurtzite structure. The crystallite size calculated by Debey-Scherrer formula is in the range of 8.03–13.06nm. The absorbance spectra signify that La doping can increase the optical bandgap of ZnO nanoparticles. The band gap is tailored from 3.76 eV to 4.3 eV by changing La doping concentration between 0% and 10%. In addition, the effects of La doping concentrations on microstructure, thermal, optical and morphological properties are discussed.

(Received January 1, 2017;Accepted March 1, 2017)

Keywords: Polymer assisted combustion synthesis; La-doped ZnO nanoparticles; XRD; TG-DTA; UV-Vis spectroscopy; SEM and TEM.

1. Introduction

Recently, zinc oxide (ZnO) has attracted much awareness within the scientific community as a potential opto-electronic material. The properties of nanoparticles which are different from those of bulk materials have encouraged many researchers to study nanosized materials for their different applications. As a wide band gap semiconductor, ZnO has the direct-band gap of 3.37 eV at room temperature and high exciton binding energy of 60 meV [1]. The broad range of applications for Zinc Oxide (ZnO) semiconducting material comprises of UV light emitting diodes [2], varistors [3], gas sensors [4], biosensors [5], solar cells [6] and catalysts [7].

Doping with proper elements is an effective approach to alter the electronic, optical and magnetic properties of semiconductor nanocrystals.[8,9] As dopants of semiconductors, rare-earth (RE) elements have attracted intensive interests since they have a great possibility to efficiently modulate the emission in the visible range due to their unique optical properties [10].The role of the particle size, doping, impurities, and morphology is very important to these applications, which has motivated researchers to focus on the synthesis of doped and pure nanocrystalline ZnO in current years. Therefore, many methods, including sol–gel [11], thermal decomposition [12], precipitation [13], spray pyrolysis [14], hydrothermal [15], chemical vapor deposition (CVD) [16], and others, have been developed to prepare ZnO nanostructures and ceramics. Thus, although a variety of methods have been used to synthesis pure and undoped ZnO nanoparticles, it still needs

* Corresponding author:seshusai7@gmail.com

a great deal of work to explore simple and new approach with low cost to synthesis ZnO nanoparticles.

The present work describes synthesis and characterization of lanthanum doped zinc oxide nanoparticles by a facile polymer assisted combustion synthesis, using zinc nitrate as source of Zn^{2+} ions and lanthanum nitrate as source of La^{3+}ions. The preparative parameters have been optimized at initial stages of deposition. The structural, optical and morphological properties have been studied and reported here.

The mentioned method in comparison with the further methods has its own advantages, such as low-processing cost, high quality, relatively low temperature and high manufacture yield. The effects of different dopant concentrations especially on micro structural properties of the La-doped ZnO nanoparticles are discussed.

2. Experimental

2.1 Preparation of ZnO nanoparticles

Solution Combustion synthesis technique (SCS) has been known as one of the eco friendly, effective, and economic method, which is a versatile process due to synthesis of single phase, solid solution, composite as well as compound oxide phase in homogeneous, simple experiment set up and significant time saving and high purity product. The method exploits self-sustaining solid flame combustion reaction for the internal development of very short period. Fuel to oxidizer ratio is very crucial and effective amount in this method; it can change the properties of product [17].

$$\psi = \frac{\text{oxidizing (or) reducing elements in fuel}}{\text{all oxidizing and reducing elements in oxidizer}}$$

La-doped Zinc oxide ($La_xZn_{1-x}O$) nanoparticles were successfully prepared by polymer assisted combustion synthesis. Metal nitrate sources with Lanthanum nitrate ($La(NO_3)_3.6H_2O$, MERCK, India) and Zinc nitrate hexahydrate ($Zn(NO_3)_2.6H_2O$, MERCK, India) salts were used as starting materials for the synthesis of La-doped Zinc oxide ($La_xZn_{1-x}O$, *x= 0.0, 0.02, 0.04, 0.06, 0.08 and 0.1*) nanoparticles. La and Zn nitrate salts were dissolved in distilled water with appropriate amounts. The fuel, Glycine ($C_2H_5NO_2$), is assisted with polyvinyl alcohol, was dissolved in water keeping ratio $\psi = 1$, the individual solutions were mixed by magnetic stirring. The mixture added in a Pyrex glass beaker is put on the hot plate. As the temperature reached 100^0C, water started to boil and evaporate from the solution, which increased solution viscosity significantly, during which the mixture trapped with fire. Finally light weight white powder is remained as a residue. Then the powder is calcined for two hours at 400^0C.

2.2. Characterization

The crystal structures of the calcined samples were characterized by powder X-ray diffraction (XRD) using an (Bruker D8 ,Advance, Germany) X-ray diffractometer . XRD was performed within the range of $20^0 \leq 2\theta \leq 80^0$ by using CuKα as radiation (1.5406 Å) in configuration The thermal properties of the calcined samples were characterized by thermogravimetric-differential thermal analysis (TG-DTA) (SII EXSTAR-6000, TG/DTA-6300). The optical properties of the samples were characterized by UV-Vis Spectroscopy (Systronics, India) with a wavelength range of 200-800 nm. The particle size and morphology of the calcined powders were characterized by transmission electron microscopy (Tecnai G2 F20 S-TWIN FEI Transmission Electron Microscope operating at 200 kV).

3. Results and discussion

3.1 XRD analysis

The XRD patterns of the as-prepared samples of La-doped ZnO nanoparticles *(x=0.0, 0.02, 0.04, 0.06, 0.08, 0.1)* in the range of 2θ = 20^0–80^0 are as shown in Fig. 1. All evident peaks could be indexed as the ZnO hexagonal wurtzite structure (JCPDS data card no: 36- 1451). No further peaks were detected related to La, or La_2O_3 other similar compounds. A negligible shift also occurred in peaks for the samples doped with a different amount of La in the ZnO matrix compared to the pure ZnO nanoparticles. This shift also corresponded to the strain of the compounds and replacement of some Zn^{2+} with the La^{3+} in each compound due to their different ionic radius.

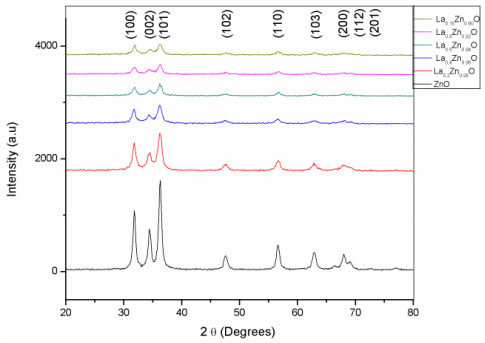

Fig. 1. XRD pattern of the as prepared La-doped ZnO nanoparticles

Wurtzite lattice parameters such as the values of d, the distance between adjacent planes in the Miller indices (h k l) (calculated from the Bragg equation, λ = 2dsin θ), lattice constants a, b, and c, and unit cell volumes were calculated using the Lattice Geometry equation [18]. The lattice parameters of the powders calcined at different temperatures are summarized in Table

$$\frac{1}{d^2}=\frac{4}{3}\left(\frac{h^2+hk+k^2}{a^2}\right)+\frac{l^2}{c^2} \quad (1)$$

$$V=\frac{\sqrt{3}a^2c}{2}=0.866a^2c \quad (2)$$

Applying the Scherer formula [11]and the full width at half maximum (FWHM) to the all planes ,average values of crystallite sizes have been calculated for the ZnO and La-doped ZnO nanoparticles in the range of 8.03–13.06 nm for the synthesized particles .

The crystallite size of the La-doped ZnO nanoparticles was determined by the X-ray line broadening method using the Scherer equation: $=\frac{k\lambda}{\beta_D cos\theta}$, where D is the crystallite size in nanometers, λ is the wavelength of the radiation (1.54056 A ° for CuK_α radiation), k is a constant equal to 0.94, β_D is the peak width at half-maximum intensity, and θ is the peak position.

The lattice strain (ε) has been determined by using the tangent formula.

$$\varepsilon_{av}=\frac{\beta}{4\,tan\theta} \quad (3)$$

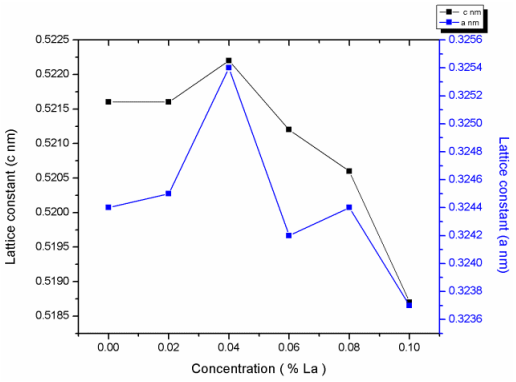

Fig. 2. Concentration of La (%) Vs Lattice constants (a and c) of La-doped ZnO nanoparticles

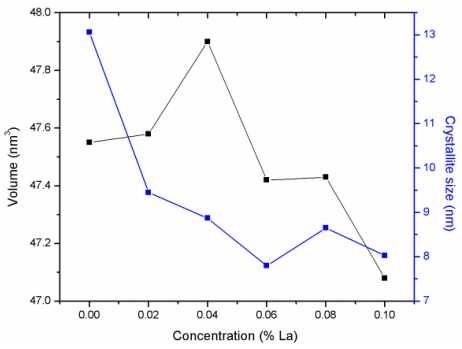

Fig.3. Concentration of La (%) Vs Crystallite size and Volume of La-doped ZnO nanoparticles

In Fig.2. it was observed with increase of Lanthanum concentration a slight increase in lattice parameters is observed up to 0.4 % La doping in ZnO matrix and a sudden decline in lattice parameters *a* and *c* is observed after increase in La doping. From Fig.3.it was noticed that, cell volume as well as crystallite size is decreased due to increase in La dopant concentration.

Products of combustion synthesis are highly porous. The density of La-doped ZnO nanoparticles was determined by the XRD. The percentage of porosity was calculated from the measured and theoretical density, according to the following equation.

$$\text{Porosity}(P) = (1 - \frac{D_x}{D_t}) \quad (4)$$

Where D_t is theoretical density, and D_x is the density of the samples measured using XRD. Using equation (4) the porosity values are calculated.

Table 1.Crystallite size, Average lattice strain, Lattice parameters (a and c), Cell Volume of La-doped ZnO nanoparticles calculated from XRD

Sample	**Crystallite Size (Debye method) nm**	**Average lattice strain ε**	**Lattice parameters (*a*) nm**	**Lattice parameters (*c*) nm**	**c/a**	**Volume $(nm)^3$**
ZnO	13.06	0.41970	0.3244	0.5216	1.6078	47.55
$La_{0.02}Zn_{0.98}O$	9.45	0.58339	0.3245	0.5216	1.6073	47.58
$La_{0.04}Zn_{0.96}O$	8.87	0.63334	0.3254	0.5222	1.6047	47.90
$La_{0.06}Zn_{0.94}O$	7.80	0.61092	0.3242	0.5212	1.6076	47.42
$La_{0.08}Zn_{0.92}O$	8.65	0.64357	0.3244	0.5206	1.6048	47.43
$La_{0.10}Zn_{0.90}O$	8.03	0.70573	0.3237	0.5187	1.6024	47.08

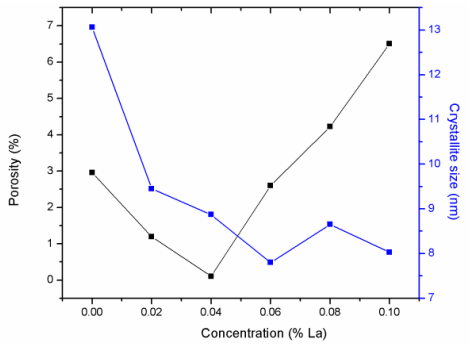

Fig.4. Concentration of La (%) Vs Crystallite size and Porosity of La-doped ZnO nanoparticles

It is clear from Fig.4.in samples porosity has no significance up to x = 0.04 doping concentrations and from x =0.06-0.1 it showed increase in porosity uniformly with La doping. This can be explained by taking the density of ZnO (5.675 gm/cc). In table I, the changes in the crystallite size, average lattice strain, lattice parameters (*a* and *c*), cell volume are attributed to the incorporation of La ions into the ZnO lattice. In table II, the Porosity of La-doped ZnO nanoparticles calculated from XRD is reported.

Table 2. The Porosity of La-doped ZnO nanoparticles calculated from XRD.

Sample	Porosity (%)
ZnO	2.96089
$La_{0.02}Zn_{0.98}O$	1.19723
$La_{0.04}Zn_{0.96}O$	0.10112
$La_{0.06}Zn_{0.94}O$	2.600586
$La_{0.08}Zn_{0.92}O$	4.221753
$La_{0.10}Zn_{0.90}O$	6.504107

3.2.Thermal Analysis

Thermogravimetric analysis is one of the mainly used techniques to observe the composition and structural dependence on the thermal degradation of a material. Fig.5.shows the results of thermogravimetric analyses (TGA, DTG, and DTA) of the La-doped ZnO nanoparticles. In all the samples of La doped ZnO nanoparticles from *x= 0.0,0.02,0.04,0.06,0.08 and 0.1* the sharp DTG peak centered at 400^0 C to 450 ^{0}C accompanied by a strong exothermic peak in the DTA curve should arise from the oxidation and decomposition correspondingly significant weight loss is observed in TG analysis. A large exothermic peak is exhibited at 400^0- 450^0C, due to the crystallization of ZnO. Therefore, the crystallization of ZnO nanoparticles occurred at these particular temperatures. In TG analysis for La doped ZnO nanoparticles there is significant weight losses observed in the samples which shows the sample is high purity in nature.

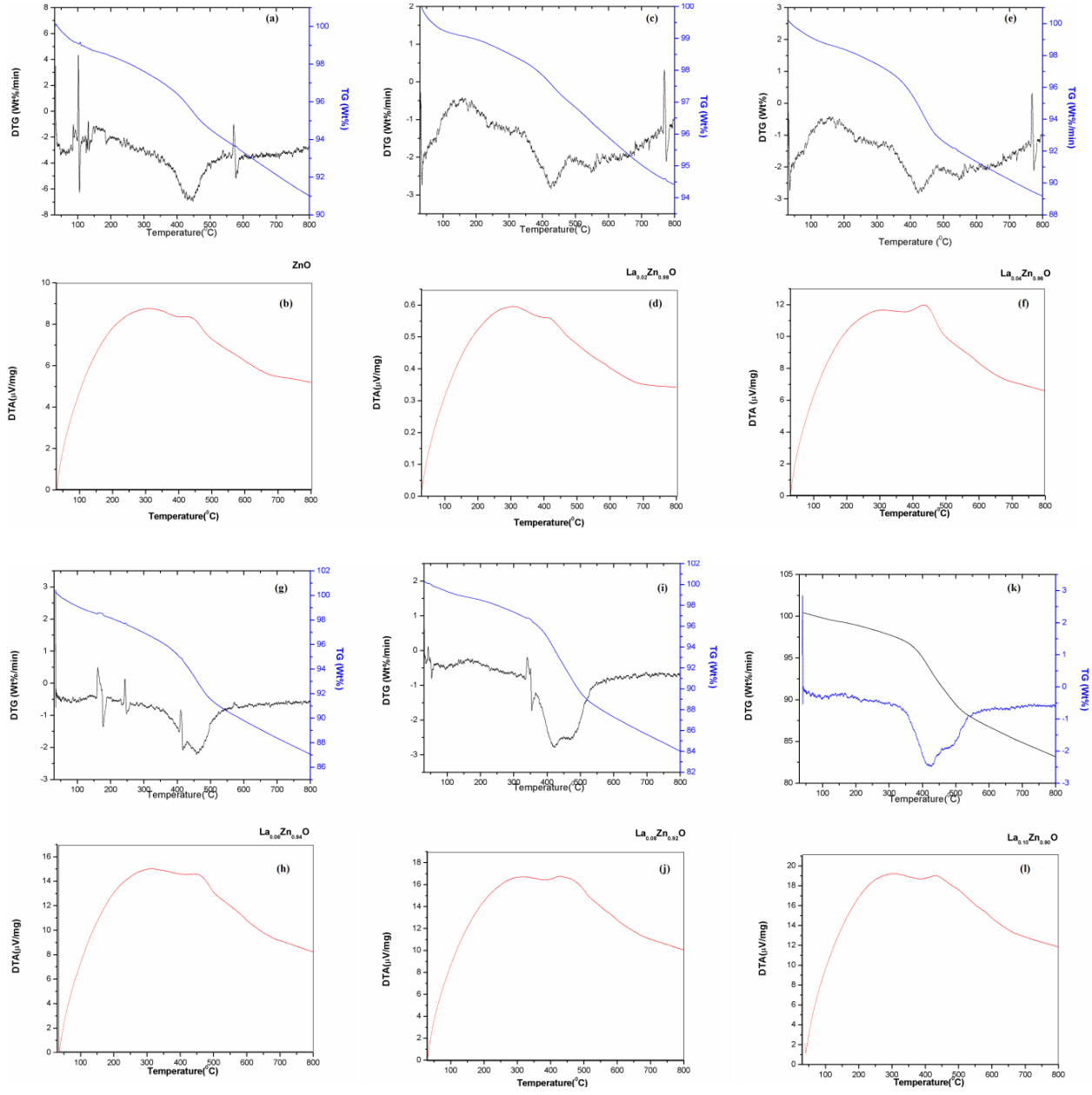

Fig.5. TG, DTA and DTG curves of La-doped ZnO nanoparticles for various concentrations (x = 0.0 to 1.0)

3.3. UV- Vis Spectroscopy

Fig. 6.Shows the absorption spectra (a) and corresponding calculated band gap (b) of samples, in which the band gap is estimated from the optical absorption spectra. For a direct band gap semiconductor, the relationship of the absorption coefficient and the band gap energy can be described by the following equation:

$$(\alpha h\nu)^{\frac{1}{2}} = A(h\nu - E_g) \quad (6)$$

where A is a constant, and a, $h\nu$ and E_g are denoted as the absorption coefficient, photon energy and optical band gap, respectively. The optical band gap (Eg) is obtained by plotting $(\alpha h\nu)^2$ versus ($h\nu$) and extrapolating the tangent of the curve to $(\alpha h\nu)^2$. It can be clearly seen that the absorption edge exhibits a blue shift and the band gap increases with increasing the La loading,

which can be ascribed to the strong interaction between the surface oxides of Zn and La, as well as the quantum size effect and Burstein–Moss effect. [19] The band gap is tailored from 3.76 eV to 4.3 eV by changing La doping concentration between 0% and 10%.

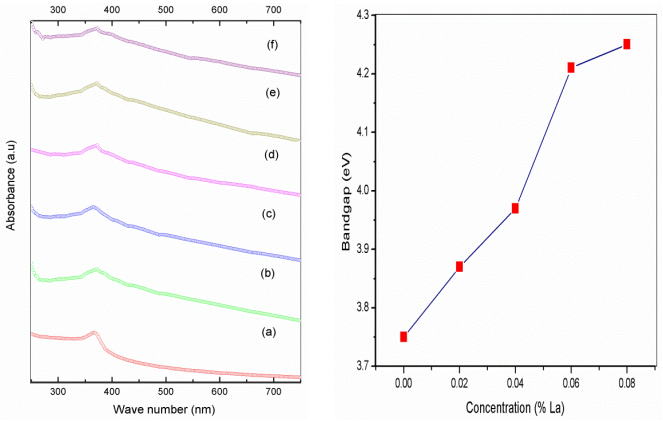

a) b)

Fig. 6.a) Absorbance of the La-doped ZnO nanoparticles with concentration, b) Bandgap of the La-doped ZnO nanoparticles with concentrations

3.4 Scanning Electron Microscopy

La-dopedZnO nanoparticles morphology was studied by SEM. Figures 7 (a) to (f) shows the high and low magnification SEM micrographs respectively. The morphology of the samples obtained by polymer assisted combustion route were of high porosity due excess of fuel corroboration.

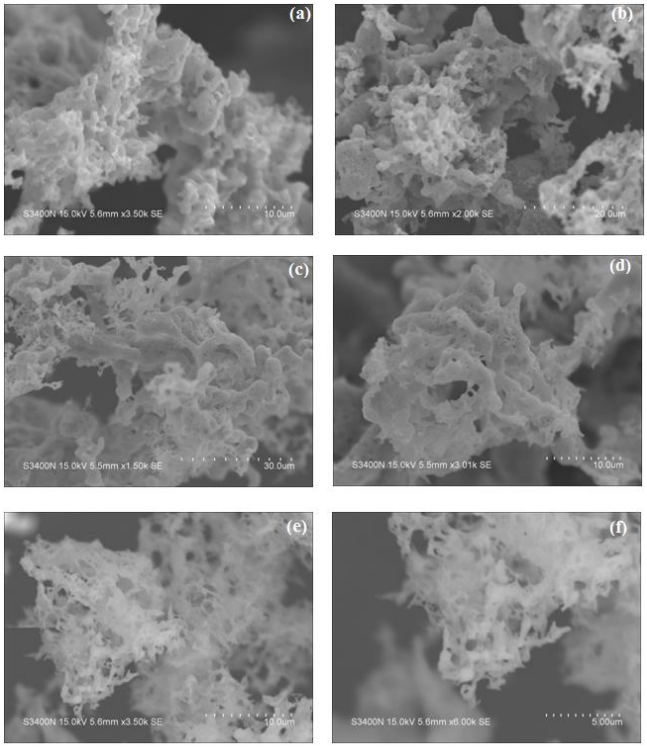

Fig. 7.SEM images of a, b, c, d, e and f for La-doped ZnO nanoparticles

3.5. Scanning Electron Microscopy - EDX Analysis

In order to reveal that the La has been doped in the structure of ZnO nanoparticles, energy dispersion X-ray (EDX) analysis was used to quantify the doping content in La-doped ZnO nanoparticles. The EDX results are presented in Fig.8 (a),(b) and (c) for un-doped ZnO nanoparticles and La-doped ZnO *(for x = 0.02,0.04)* nanoparticles, which reveal that the La element has been incorporated into the structure of ZnO nanoparticles. Also, we can see that the nanoparticles are mostly composed of Zn, La, O, and C elements. The actual molar ratio of La/Zn in the doped ZnO nanoparticles was determined. The analytical data are given in corresponding Figures from which we can see that the actual molar ratios in the final products are approximately close to the original prescribed ones. Hence, we can identify that the La element has been incorporated into the ZnO nanoparticles successfully. Figure a, b, c shows the energy-dispersive X-ray spectroscopy of La-doped ZnO nanoparticles. The EDX confirmed the presence of both La and Zn elements in the sample. It also confirmed the successful doping of La into ZnO. The weight percentage and intensity of elements are given in the Fig 8.a. to Fig 8.c.

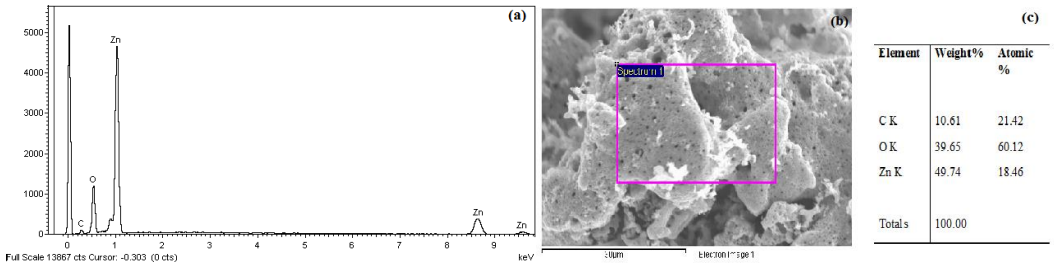

Fig.8. a. SEM – EDX analysis of pure ZnO nanoparticles

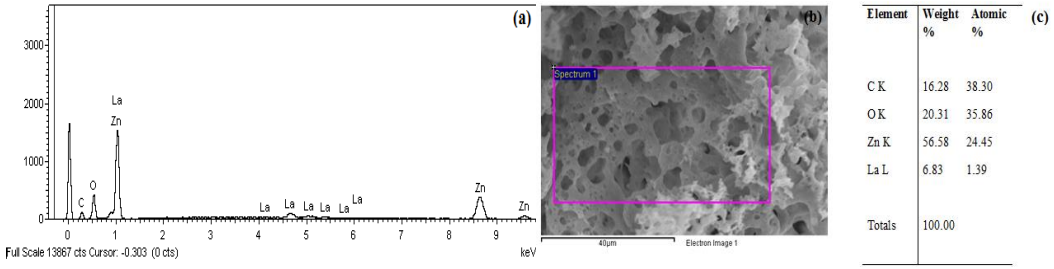

Fig.8. b. SEM – EDX analysis of $La_{0.04}Zn_{0.96}O$ *nanoparticles*

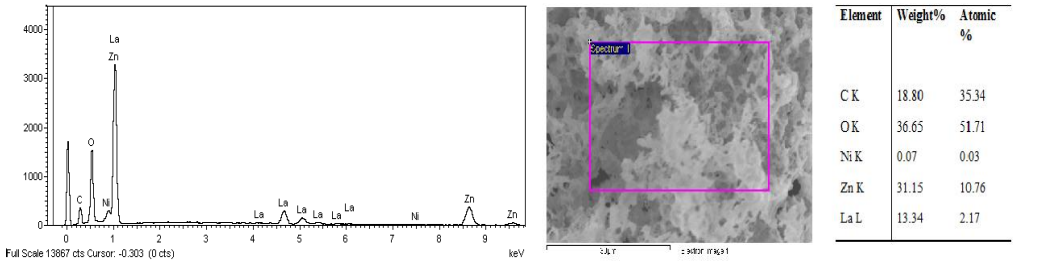

Fig.8. c. SEM – EDX analysis of $La_{0.10}Zn_{0.90}O$ *nanoparticles*

3. 6.Transmission Electron Microscopy

A typical TEM micrograph of the ZnO and La-doped ZnO nanoparticles obtained by polymer assisted combustion synthesis method at different magnifications is shown in Fig. 9. The powder consists of particles less than 20 nm in size. The morphology of pure ZnO nanoparticles clearly indicates the formation of presence of hexagonal wurzite structure. Fig. 3 shows the

Selected Area Electron Diffraction pattern of the pure ZnO nanopowder. Sharp diffraction rings appear in the diffraction pattern and strong diffraction spots exist in these rings. The diffraction pattern corresponds with zinc oxide. As shown in Fig. 3, no amorphous phase can be detected in the diffraction pattern.

The powder consist particles further less than 15 nm. The morphology of La-doped ZnO nanoparticles indicates the deformation in hexagonal wurzite structure to spherical due to the addition of La doping. Fig.9. shows the Selected Area Electron Diffraction pattern of the pure ZnO nanopowder. Sharp diffraction rings appear in the diffraction pattern and strong diffraction spots exist in these rings. The diffraction pattern corresponds with zinc oxide. As shown in Fig. 9. , no amorphous phase can be detected in the diffraction pattern. The pattern of diffracted rings and the lattice planes indicates that the crystallinity becomes weaker as the content of La increases, which is in good agreement with the XRD results.

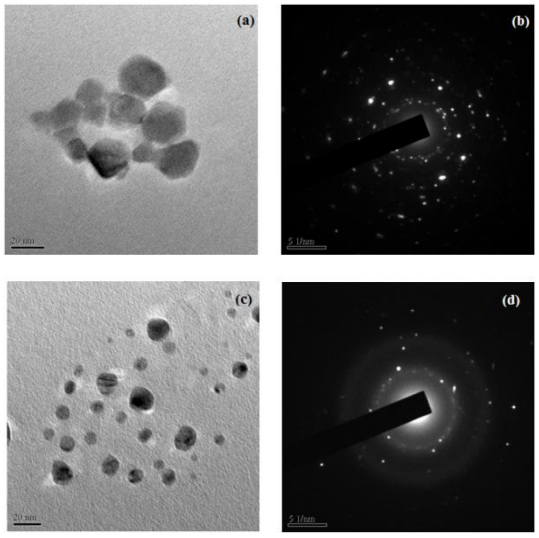

Fig.9. TEM analysis of pure ZnO and $La_{0.04}Zn_{0.96}O$ *nanoparticles*

4. Conclusions

La-doped ZnO nanoparticles have been effectively synthesized by a polymer assisted combustion synthesis route. The XRD results indicated that the synthesized La-dopedZnO nanoparticles had the pure wurtzite structure without any impurities and secondary phases. The crystallite sizes decreased with increase in the La concentration. The reduction in average crystalline size and the slight shift of XRD peaks of La-doped ZnO indicated that La has really doped into the ZnO structure. From TG/DTA analysis crystallization of La doped ZnO nanoparticles is observed in the temperature range of 400^0-450^0C.The optical band gaps were found to increase with the increase in doping concentrations. SEM indicated, the obtained samples are having high porosity due excess of fuel corroboration. From TEM analysis it is observed that the obtained pure ZnO and $La_{0.04}Zn_{0.96}O$ nanoparticles are of crystalline in nature. TEM photographs indicated that the grain size of undoped ZnO is bigger than the La-doped ZnO which is due to the limitations of grain growth upon La doping.

Acknowledgements

The authors are thankful to Sophisticated Analytical Instrument Facility - North-Eastern Hill University, Shillong and University of Hyderabad, Hyderabad for their valuable help regarding TEM, SEM and EDX characterizations.

References

[1] M. Li ,H. Bala, X.LvX, X.Ma, F.Sun, L.Tang , Mater Lett . **61**, 690 (2007).
[2] Yoshitake Masuda, Naoto Kinoshita,Fuyutoshi Sato, KunihitoKoumoto, Cryst. Growth Des. **6**, 75(2006).
[3] M. Singhai, V. Chhabra, P. Kang, D.O. Shah, Mater. Res.Bull. **32**, 239 (1997).
[4] Hongyan Xu, Xiulin Liu, Deliang Cui, Mei Li, Minhua Jiang, Sensor. Actuat. B. **114**, 301 (2006).
[5] Ahmad Umar, M.M. Rahman, Mohammad Vaseem,Yoon-Bong Hahn, Electrochem. Commun.**11**, 118, (2009).
[6] Elena Guillén, EnekoAzaceta, Laurence M. Peter, ArnostZukal, Ramón Tena-Zaera and Juan A. Anta, Energy Environ. Sci., **4,** 3400 (2011).
[7] ZohrehMirjafary, HamdollahSaeidian, AzamSadeghi, FirouzMatloubiMoghaddam, Catal.Commun.**9**, 299 (2008).
[8] D. J. Norris, A. L. Efros and S. C. Erwin, Doped Nanocrystals, Science, **319**, 1776 (2008).
[9] Y. C. Cao, Impurities Enhance Semiconductor Nanocrystal Performance, Science **332**, 48-49 (2011).
[10] F. Wang, X. Liu, Chem. Soc. Rev., **38**, 976 (2009).
[11] A. Muthuvinayagam, Boben Thomas, P. Dennis Christy, R. Jerald Vijay, T. Manovah David, P. Sagayaraj, Arch. App. Sci. Res. **3**, 256 (2011).
[12] Hashem Shahroosvand and MahsaGhorbani-asl, CrystEngComm, **14**, 8199 (2012).
[13] ZahraMonsefKhoshhesab, Mohammad Sarfaraz& Mohsen AsadiAsadabad, Synth. React. Inorg. Me. **41,** 814, (2011).
[14] Sang Duck Lee, Sang-Hun Nam, Myoung-Hwa Kim, Jin-Hyo Boo, Physics Procedia, **32**, 320, (2012).
[15] SunandanBaruah, Joydeep Dutta, Sci. Technol. Adv. Mater.**10**, 013001 (2009).
[16] Hong Wan, Harry E. Ruda, Journal of Materials Science: Materials in Electronics **21,** 1014,(2010).
[17]Singanahally T. Aruna , Alexander S. Mukasyan, Current Opinion in Solid State and Materials Science **12**, 44, (2008).
[18] B.D. Cullity, Elements of X-ray Diffraction (Addison- Wesley Publishing Company Inc.: California: (1956).
[19] A. Y. Oral, Z. B. Bahsi, and M. H. Aslan, Appl. Surf. Sci. **253**, 4593, (2007).